Received: 11 October 2018 | Revised: 1 January 2020 | Accepted: 25 December 2020

DOI: 10.1111/jnc.15294

ORIGINAL ARTICLE

Journal of Neurochemistry JNC The Official Journal of the International Society for Neurochemistry WILEY

Late post-natal neurometabolic development in healthy male rats using ^{1}H and ^{31}P magnetic resonance spectroscopy

Veronika Račkayová[1,2,3] | Dunja Simicic[1,2,3] | Guillaume Donati[3] | Olivier Braissant[4] | Rolf Gruetter[3] | Valérie A. McLin[5,6] | Cristina Cudalbu[1,2]

[1]CIBM Center for Biomedical Imaging, Lausanne, Switzerland

[2]Animal Imaging and Technology, Ecole Polytechnique Federale de Lausanne (EPFL), Lausanne, Switzerland

[3]Laboratory of Functional and Metabolic Imaging (LIFMET), Ecole Polytechnique Federale de Lausanne (EPFL), Lausanne, Switzerland

[4]Service of Clinical Chemistry, University of Lausanne and University Hospital of Lausanne, Lausanne, Switzerland

[5]Swiss Pediatric Liver Center, University Hospitals Geneva, Geneva, Switzerland

[6]Department of Pediatrics, Gynecology, and Obstetrics, University of Geneva Medical School, Geneva, Switzerland

Correspondence
Cristina Cudalbu, CIBM Center for Biomedical Imaging, Animal Imaging and Technology, Ecole Polytechnique Fédérale de Lausanne (EPFL), EPFL ENT-R CIBM-AIT, Station 6, CH-1015 Lausanne, Switzerland.
Email: cristina.cudalbu@epfl.ch

Funding information
Schweizerischer Nationalfonds zur Förderung der Wissenschaftlichen Forschung, Grant/Award Number: 310030_173222; EU: FP7-PEOPLE-2012-ITN, Grant/Award Number: 316679 - TRANSACT

Abstract

Brain metabolism evolves rapidly during early post-natal development in the rat. While changes in amino acids, energy metabolites, antioxidants or metabolites involved in phospholipid metabolism have been reported in the early stages, neurometabolic changes during the later post-natal period are less well characterized. Therefore, we aimed to assess the neurometabolic changes in male Wistar rats between post-natal days 29 and 77 (p29-p77) using longitudinal magnetic resonance spectroscopy (MRS) in vivo at 9.4 Tesla. ^{1}H MRS was performed in the hippocampus between p29 and p77 at 1-week intervals ($n = 7$) and in the cerebellum between p35 and p77 at 2-week intervals ($n = 7$) using the SPECIAL sequence at ultra-short echo-time. NOE enhanced and ^{1}H decoupled ^{31}P MR spectra were acquired at p35, p48 and p63 ($n = 7$) in a larger voxel covering cortex, hippocampus and part of the striatum. The hippocampus showed a decrease in taurine concentration and an increase in glutamate (with more pronounced changes until p49), seemingly a continuation of their well-described changes in the early post-natal period. A constant increase in myo-inositol and choline-containing compounds in the hippocampus (in particular glycero-phosphocholine as shown by ^{31}P MRS) was measured throughout the observation period, probably related to membrane metabolism and myelination. The cerebellum showed only a significant increase in myo-inositol between p35 and p77. In conclusion, this study showed important changes in brain metabolites in both the hippocampus and cerebellum in the later post-natal period (p29/p35-p77) of male rats, something previously unreported. Based on these novel data, changes in some neurometabolites beyond p28-35, conventionally accepted as the cut off for adulthood, should be taken into account in both experimental design and data interpretation in this animal model.

Abbreviations: AHP, adiabatic half passage; Ala, alanine; Asc, ascorbate; Asp, aspartate; ATP, adenosine tri-phosphate; bHB, β-hydroxybutyrate; Cr, creatine; CRLB, Cramer-Rao lower bounds; GABA, γ-aminobutyric acid; Glc, glucose; Gln, glutamine; Glu, glutamate; GOT, L-aspartate:2-oxoglutarate aminotransferase, GPC, glycerophosphocholine; GPE, glycerophosphoethanolamine; GS, glutamine synthetase; GSH, glutathione; Ins, myo-inositol; Lac, lactate; MRS, magnetic resonance spectroscopy; NAA, N-acetylaspartate; NAAG, N-acetylaspartylglutamate; NAD, nicotinamide adenine dinucleotide; NOE, nuclear Overhauser effect; OVS, outer volume suppression; PCho, phosphocholine; PCr, phosphocreatine; PE, phosphoethanolamine; Pi_{alk}, alkaline inorganic phosphate; Pi_{in}, intracellular inorganic phosphate; RRID, Research Resource Identifier (see scicrunch.org); Scyllo, scyllo-inositol; Tau, taurine; tCho, total choline; tCr, total creatine; VAPOR, variable power and optimized relaxation delays; VOI, volume of interest.

Veronika Račkayová and Dunja Simicic these authors contribution equally to this work.

KEYWORDS
in vivo ^{1}H MRS, in vivo ^{31}P MRS, late post-natal brain development, neurochemical profile during development, Wistar rats

1 | INTRODUCTION

Post-natal brain development in rats is characterized by temporal changes in the concentrations of its metabolites. These changes have been studied in detail mainly at late embryonal and early post-natal stages until post-natal day 28 (p28) or p35; beyond this time-point rats are considered adults (Agrawal et al., 1971; Bayer & McMurray, 1967; Burri et al., 1990; Huxtable et al., 1989; Terpstra et al., 2010; Tkáč et al., 2003). These studies have shown that the most prominent changes in the concentrations of metabolites during brain development include increases in N-acetyl-aspartate, creatine and phosphocreatine. A decrease in taurine and variations in amino acids involved in neurotransmission (glutamine, glutamate, γ-aminobutyric acid) were also observed. Next, variations in phospholipids and metabolites involved in phospholipid metabolism such as different choline- and ethanolamine-containing compounds were reported in these studies. Also, an increase in myo-inositol and fluctuations in antioxidants were clearly established. Finally, various changes in the transport of metabolic substrates and in the metabolism of glucose, fatty acids, ketone bodies and lactate have been reported (Erecinska et al., 2004; Mckenna et al., 2015). These changes have been linked to the following metabolic processes: a decrease in ketone body utilization after the suckling period (about p21), a decrease in the rate of lactate transport through brain capillaries, an increase in glucose transport and utilization since birth, and enzymatic maturation after p30.

In other mammals and humans, the nervous system develops over a long period of time. In the rat, though most of the post-natal developmental changes happen within the first three post-natal weeks, some aspects of cell differentiation, synaptogenesis, gliogenesis and myelination continue beyond p45 (Rice and Barone 2000; Semple et al., 2013). In addition, synaptogenesis and myelination continue into adulthood (Rice and Barone 2000; Erecinska et al., 2004) and happen in a region-dependant manner (Semple et al., 2013). These later changes are of interest given the importance of the rat model in understanding brain physiology and modelling human disease.

The hippocampus and cerebellum are particularly compelling to study late brain development and differentiation. Certain developmental processes occur later and at a slower rate than in other brain regions. In particular, the hippocampal dentate gyrus and cerebellum are two areas remarkable for extended neurogenesis (Bayer et al., 1993): while it reaches a maximum at p12-15, it continues slowly into adulthood in both the hippocampus and cerebellum (Altman, 1972a, 1972b, 1972c; Altman & Das, 1965, 1966). The cerebellum is chronologically also one of the last brain regions to benefit from mature enzymes involved in glycolysis and in the tricarboxylic acid cycle (Leong & Clark, 1984a, 1984b).

Therefore, the purpose of this study was to evaluate the neurometabolic changes of healthy male rats during the late post-natal period (p29-p77) in the hippocampus, cerebellum and in a larger voxel covering cortex, hippocampus and part of the striatum. The rationale was to study the equivalent of childhood and adolescence in humans, as little is known about precise timing of later post-natal changes. Using ^{1}H and ^{31}P MRS at high magnetic fields (i.e. 9.4T), we aimed to describe a time course of metabolic changes in the brain of young adult rats. These non-invasive and complementary techniques allow the assessment of brain metabolites involved in neurotransmission, osmoregulation, cellular redox state, phospholipid and energy metabolism in vivo and with high precision.

2 | METHODS

2.1 | Study design

All animal experiments were conducted according to federal and local ethical guidelines, the protocols were approved by the local Committee on Animal Experimentation for the Canton de Vaud, Switzerland (VD 2761) and the study was not pre-registered.

Thirty-five Wistar male rats (n = 35 animals) were used in the study: seven rats for ^{1}H MRS measurements in hippocampus at p29, p43, p57, p71; seven rats for ^{1}H MRS measurements in hippocampus at p35, p49, p63, p77; seven rats for ^{1}H MRS measurements in cerebellum at p35, p49, p63, p77; and seven rats for ^{31}P MRS at p35, p49, p63. Five groups of rats (n = 7 animals per group) were used in order to decrease the exposure of each animal to anaesthesia (i.e. one group of rats per MRS experiment and per brain region). Because of technical reasons, ^{1}H MRS data in cerebellum at p35 and ^{31}P MRS data at p63 were acquired only on six rats. The last group of rats (n = 7) was scanned only once at p77 in the hippocampus using ^{1}H MRS and was compared with the rats scanned longitudinally at the same time point to assess the potential effects of recurrent anaesthesia.

Wistar Han IGS dams (Crl:WI(Han)) and their male pups were obtained on p10/p11 (rats that started the MRS measurements on p29) or on p16/p17 (all the other rats) from Charles River laboratories (L'Arbresle, France). All animals were weaned at p21.

During the MR experiments, animals were kept under 1.5%–2% isoflurane anaesthesia (~50% air and ~50% oxygen, Attane™ Isoflurane ad us. vet., Piramal Healthcare) with respiration rate maintained at 60–70 breaths/min and body temperature at 37.5–38.5°C. Animals were kept in the animal facility with 12 hr/12 hr light/dark cycle in a cage type E 1050 cm^2 (2–3 rats per cage). Standard rat chow and water were available ad libitum for the duration of study.

2.2 | MRS

All MR experiments were performed on a horizontal actively shielded 9.4 Tesla system (Magnex Scientific) interfaced to a Varian Direct Drive console. The magnet characterized by a 31 cm horizontal bore is equipped with a 12 cm inner-diameter actively shielded gradient sets giving a maximum gradient strength of 400 mT/m in 120 μs. Eddy currents were minimized using time-dependent quantitative eddy current field mapping (Terpstra et al., 1998). Two home-built coils were used, described in the corresponding sections below. The volume of interest (VOI) was positioned on axial and sagittal anatomical T_2-weighted images (multislice turbo-spin-echo sequence, repetition time TR = 4 s, effective echo time TE_{eff} = 52 ms, echo train length = 8, field of view = 23 × 23 mm^2, slice thickness = 1 mm, 2 averages, 256 x 256 image matrix). The static magnetic field homogeneity was adjusted using first- and second-order shims by FAST(EST) MAP (Gruetter, 1993; Gruetter & Tkác, 2000).

2.2.1 | ^{1}H MRS

A quadrature surface coil was used as a transceiver (loops diameter = 14 mm) to measure the VOI placed in dorsal hippocampus (2 × 2.8 × 2 mm^3) or cerebellum (2.5 × 2.5 × 2.5 mm^3). Localized spectra were acquired with SPECIAL spectroscopy sequence (TE = 2.8 ms, TR = 4 s, 160 averages) (Mlynárik et al., 2006). Outer volume suppression (OVS) was interleaved with water signal suppression consisting of RF pulses with variable power and optimized relaxation delays (VAPOR) (Tkáč et al., 1999).

LCModel (Provencher, 2001) (RRID:SCR_014455) was used for spectral fitting and metabolite concentrations calculation. The reliability of the metabolite concentration measure was estimated by Cramer-Rao lower bounds (CRLB) and only metabolites with CRLB lower than 30% were accepted for further analysis. The LCModel basis-set for spectral fitting contained a spectrum of macromolecules acquired in vivo (Cudalbu et al., 2012) and individual metabolites measured in vitro. The ultra-short echo-time ^{1}H MRS allowed the detection of the following 17 metabolites, all included in basis-set: alanine (Ala), ascorbate (Asc), aspartate (Asp), glycerophosphocholine (GPC), phosphocholine (PCho), creatine (Cr), phosphocreatine (PCr), γ-aminobutyric acid (GABA), glutamine (Gln), glutamate (Glu), glutathione (GSH), myo-inositol (Ins), lactate (Lac), N-acetylaspartate (NAA), N-acetylaspartylglutamate (NAAG), phosphoethanolamine (PE) and taurine (Tau). In addition, glucose (Glc), β-hydroxybutyrate (bHB) and scyllo-inositol (Scyllo) signals were included in the basis-set to increase the precision of quantification but their concentrations were not reliably estimated in most of the rats and thus not presented. PCho and GPC were expressed only as tCho (PCho + GPC) because of better accuracy in the estimation of their concentration as a sum. Ala, Asp and GSH were not reported in the cerebellum, since these metabolites reached CRLB higher than 30%.

Metabolite concentrations were expressed in mmol/kg_{ww} using the unsuppressed water signal from the same VOI as an internal reference, assuming 80% of water in brain tissue. Brain water content is known to change post-natally, the fastest decline takes place between p7 and p28 dropping from 88% to 80% (De Souza and Dobbing 1971; Tkáč et al., 2003). However, brain water content does not change significantly beyond p28 stabilizing at approximately 80% (De Souza and Dobbing 1971).

2.2.2 | ^{31}P MRS

For ^{31}P MRS, a home-built double-tuned surface coil consisting of a pair of ^{1}H-loops (diameter = 18 mm) in quadrature and a single ^{31}P-loop (diameter = 15 mm) coil were used as transceivers. Localized spectra were acquired using a non-selective adiabatic half passage (AHP) pulse for excitation, localized by OVS (x,z) and 1D-ISIS (y) (Mlynárik et al., 2012; Rackayova et al., 2016) (TR = 8 s, 384 avg.) in VOI = 5 × 9 × 9 mm^3 covering cortex, hippocampus and part of striatum. WALTZ-16 was used for nuclear Overhauser effect (NOE) and ^{1}H-decoupling. Quantification was performed using AMARES (jMRUI) (Vanhamme et al., 1997), fitting PE, PCho, intracellular and alkaline inorganic phosphate (Pi_{in} and Pi_{alk}), glycerophosphoethanolamine (GPE), GPC, PCr, reduced form of nicotinamide adenine dinucleotide (NADH) as a single spectral component; gamma- and alpha-phosphorus in adenosine tri-phosphate (γATP and αATP) and oxidized form of nicotinamide adenine dinucleotide (NAD^+) as doublets (two spectral components with equal amplitude and fixed chemical shift); and finally beta-phosphorus in adenosine tri-phosphate (βATP) as triplet (three spectral components with amplitude ratio 1:2:1 and fixed chemical shift). A detailed description of the prior knowledge used is provided in Table S1. ^{31}P MRS were corrected for NOE effect measured in a separate experiment and normalized for each rat using its PCr concentration from ^{1}H MRS (as previously described) acquired in VOI = 4 × 7.5 × 6.5 mm^3 centred in ^{31}P VOI (80 averages). A smaller VOI for ^{1}H MRS was used in order to reach better homogeneity of static magnetic field (to have water resonance linewidth of ≈14 Hz) and therefore clear separation of Cr and PCr peak. Only γATP was used to assess ATP concentration. In addition, the pH was estimated as described in (Lanz et al., 2017; Rackayova et al., 2016).

2.3 | Statistical analysis

Results (in the text and in figures) are presented as mean ± *SD* for each time-point or as mean ± *SD* of all time-points together if there was no change in the metabolite concentration during the observation period. Sample size calculation was not performed before starting the study and the number of animals was determined based on previous studies (Mlynárik et al., 2012; Rackayova et al., 2016; Terpstra et al., 2010; Tkáč et al., 2003). Prism 5.03 (Graphpad; RRID:SCR_002798) and Matlab (MathWorks; RRID:SCR_001622) were used for all the statistical analysis. Shapiro–Wilk normality test was used for every metabolite together with a QQ plot. Two-way

ANOVA was performed on ^{1}H MRS data in hippocampus and one way ANOVA on ^{1}H MRS data in cerebellum and on ^{31}P MRS data. The T-test was used to compare the data between single and multiple anaesthesia groups. The *F*-test and Bartlett-test were used to compare the variances and the Welch correction was applied to take into account the difference of variances when needed (i.e. Gln, GSH and Tau). Significance in all tests was attributed according to the following: $^{*}p < .05$; $^{**}p < .01$; $^{***}p < .001$; $^{****}p < .0001$ and all metabolites showing statistically significant changes passed the normality test (p value ranging between 0.07 and 0.97). Blinding and sample size calculation were not performed.

3 | RESULTS

3.1 | Weight

Figure 1 shows the increase in the rat's weight between p29 and p77.

3.2 | *Quality of ^{1}H MR and ^{31}P MR spectra acquired* in vivo

In general, ^{1}H MR spectra from hippocampus and cerebellum exhibited excellent signal to noise ratio and shimming resulted in unsuppressed water signal linewidths of 9–10 Hz and 14–16 Hz, respectively, leading to highly resolved spectra (Figure 2). The absence of contamination with extracerebral lipid peaks at 1.3–1.7 ppm confirmed the quality of signal localization, whereas the VAPOR water suppression provided a residual water signal intensity below that of NAA. Therefore, notable differences in metabolite signals were visible in the spectra (e.g. increase in tCho, Ins and decrease in Tau).

Figure 3 demonstrates the quality of the ^{31}P MRS spectra obtained during the study with a visible increase in amplitude of the GPC signal between p35 and p63. The use of OVS together with 1D-ISIS for localization ensured a flat baseline and narrow spectral lines. Shimming in a large voxel covering cortex, hippocampus and striatum resulted in unsuppressed water signal linewidths of 14–18 Hz. This, together with the use of a home-built double-tuned ^{1}H-^{31}P coil, ^{1}H-^{31}P NOE enhancement and ^{1}H decoupling resulted in a high signal to noise ratio with well-resolved spectral lines. Therefore, a good separation of phospho-monoesters and -diesters, intracellular and alkaline inorganic phosphate and oxidized and reduced form of NAD was obtained.

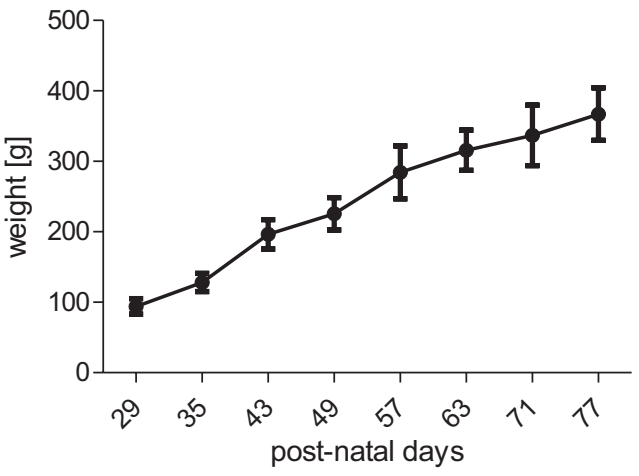

FIGURE 1 Weight of the rats between post-natal day 29 and 77. p29 ($n = 7$), p35 ($n = 7$), p43 ($n = 7$), p49 ($n = 7$), p57 ($n = 7$), p63 ($n = 7$), p71 ($n = 7$), p77 ($n = 7$),*n* represents the number of animals per group

3.3 | ^{1}H MRS in hippocampus

The time course of all metabolites measured by ^{1}H MRS in hippocampus is shown in Figure 4 and Table S2. Glu, Ins, Tau and tCho were the only metabolites showing a significant change after p29 in hippocampus.

Glu increased significantly ($p < .05$) over the observation period between p29 and p77. It increased from 8.93 ± 0.62 mmol/kg_{ww} at p29 to 10.21 ± 0.47 mmol/kg_{ww} at p49 (+14%) and reached 10.38 ± 1.01 mmol/kg_{ww} at p77. **Ins** showed a significant ($p < .0001$) increase throughout the whole study. Starting at 6.24 ± 0.49 mmol/kg_{ww} at p29, reaching 8.62 ± 1.02 mmol/kg_{ww} at p77 (+38%), with a mean increase of 0.05 mmol/kg_{ww}/day. **Tau** decreased significantly ($p < .01$) over the observation period between p29 and p77. It dropped from 8.85 ± 0.75 mmol/kg_{ww} at p29 to 7.48 ± 0.64 mmol/kg_{ww} at p49 (−15%; −0.07 mmol/kg_{ww}/day) and reached 7.28 ± 0.77 mmol/kg_{ww} at p77. **tCho** showed a significant ($p < .0001$) increase throughout the whole study. Increasing from 0.73 ± 0.16 mmol/kg_{ww} at p29 to 1.12 ± 0.12 mmol/kg_{ww} at p77 (+53%), with a mean increase of 0.008 mmol/kg_{ww}/day. No significant cross effects (time versus group) were observed in two way ANOVA analysis.

3.4 | ^{1}H MRS in cerebellum

The time course of all metabolites measured by ^{1}H MRS in the cerebellum is shown in Figure 5 and Table S3. **Ins** was the only metabolite showing a significant ($p < .0001$) change between p35 and p77 in the cerebellum. It increased from 7.17 ± 0.73 mmol/kg_{ww} at p35 to 9.02 ± 0.68 mmol/kg_{ww} at p77 (+26%), with a mean increase of 0.05 mmol/kg_{ww}/day, akin to the changed measured in the hippocampus.

3.5 | ^{31}P MRS

Figure 6 and Table S4 show the evolution of all brain metabolites measured by ^{31}P MRS between p35 and 63. Only **GPC** showed a significant increase ($p < .05$) between p35 and p63, increasing from 0.57 ± 0.12 mmol/kg_{ww} to 0.82 ± 0.20 mmol/kg_{ww} (+44%), with a mean increase of 0.009 mmol/kg_{ww}/day, in agreement with the

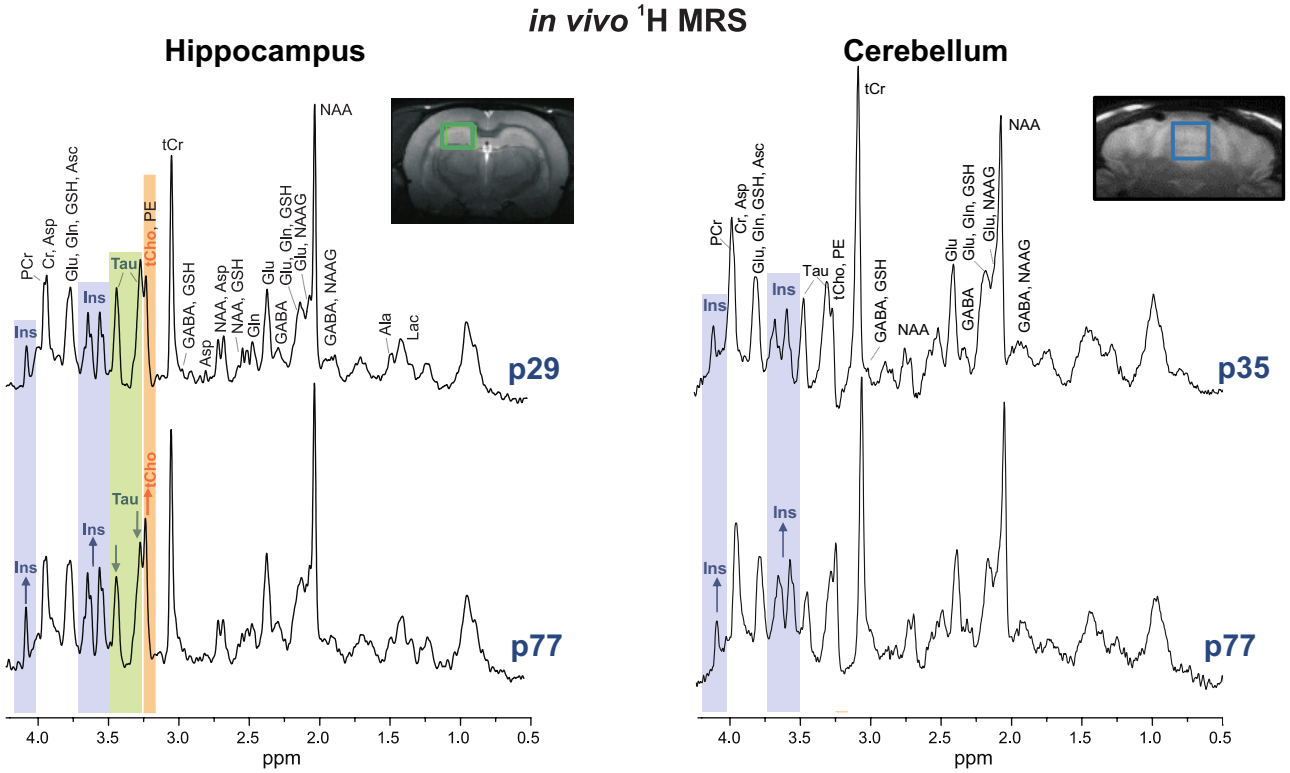

FIGURE 2 **In vivo ^{1}H MRS spectra acquired at 9.4T in the hippocampus and cerebellum in a rat at post-natal day 29 (p29)/ 35 (p35) and p77** with a visible increase in myo-Inositol (Ins, blue) and total choline (tCho, orange) resonance and decrease in taurine (Tau, green). Alanine (Ala), ascorbate (Asc), aspartate (Asp), creatine (Cr), phosphocreatine (PCr), γ-aminobutyric acid (GABA), glutamine (Gln), glutamate (Glu), glutathione (GSH), lactate (Lac), N-acetylaspartate (NAA), N-acetylaspartylglutamate (NAAG), phosphoethanolamine (PE)

increase in tCho (PCho + GPC) measured by ^{1}H MRS in hippocampus. All the other metabolites measurable by ^{31}P MRS showed only slight variations and did not reach statistical significance. In addition, we observed a significant decrease in brain pH with age, with the strongest decrease occurring between p35 and 49 ($p < .0001$).

3.6 | Potential influence of recurrent anaesthesia on brain metabolites in the hippocampus

To assess the potential effects of recurrent isoflurane anaesthesia, the metabolite concentrations in the hippocampus at p77 in the group of rats followed longitudinally were compared to those measured in an age-matched group of rats who underwent a single ^{1}H MRS measurement in the hippocampus at p77 only. No difference in the concentrations of brain metabolites between these two groups at p77 was measured, except for a 13% increase in tCho ($p = .04$) (Figure S1).

4 | DISCUSSION

This study reports significant changes in brain metabolites of rats during the late post-natal period (p29-p77), something, to the best of our knowledge, not shown previously with such resolution. All metabolite concentrations measured at p29 in the hippocampus were in close agreement with literature values obtained at p28 in the hippocampus in similar conditions (Terpstra et al., 2010; Tkáč et al., 2003). Our study revealed that after p29 Glu, Tau, tCho and Ins showed significant changes in the hippocampus. Glu showed an increase and Tau a decrease mainly until p49. tCho and Ins increased throughout the study from p29 to p77. This increase in tCho was in line with the increase in GPC measured by ^{31}P MRS in volume covering cortex, hippocampus and striatum. The only metabolite showing a significant change between p35 and p77 in the cerebellum was Ins, which increased during the observation period.

4.1 | Metabolites involved in neurotransmission

Post-natal changes in Gln, Glu, Asp and GABA are probably linked with the maturation of enzymes involved in neurotransmission processes and enzymes involved in amino-acid metabolism. In addition, changes in the ratios between glial cells, excitatory and inhibitory neurons could also play a role (Bandeira et al., 2009).

According to Bayer & McMurray, (1967), brain glutamine synthetase (GS) activity (measured in the whole brain: cerebrum and cerebellum) increases in rats until p26 and stabilizes thereafter, which is in agreement with the increase in cerebral **Gln** concentration observed from birth to p28 by in vivo ^{1}H MRS (Tkáč

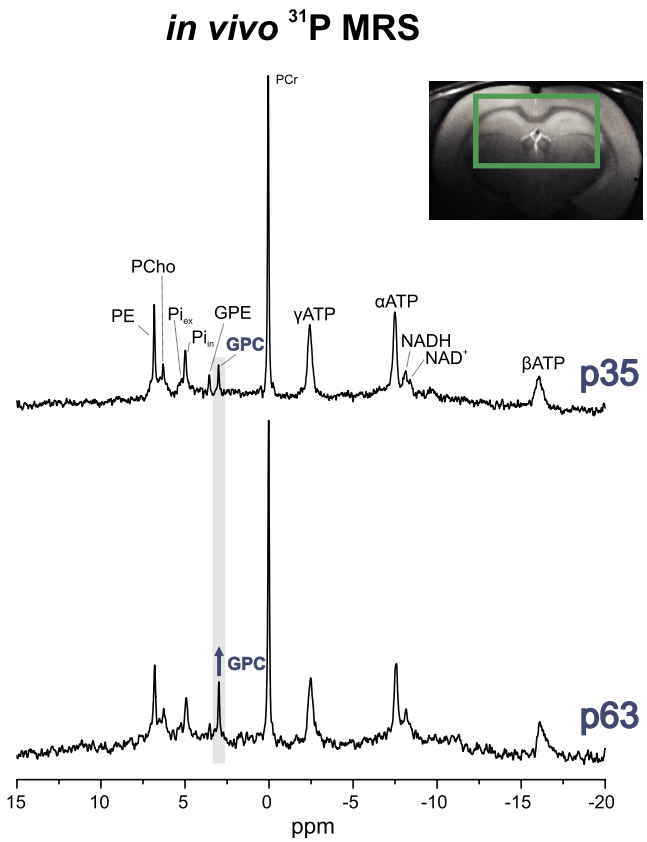

FIGURE 3 **In vivo ^{31}P MRS spectra acquired at 9.4T in the VOI = 5 × 9 × 9 mm^3 in the same rat at post-natal day 35 (p35) and p63** with a visible increase in glycerophosphocholine (GPC, grey) resonance. Phosphoethanolamine (PE), phosphocholine (PCho), alkaline and intracellular inorganic phosphate (Pi_{alk} and Pi_{in}), glycerophosphoethanolamine (GPE), phosphocreatine (PCr), gamma-, alfa- and beta-phosphorus in adenosine tri-phosphate (γATP, αATP and βATP), reduced form of nicotinamide adenine dinucleotide (NADH), oxidized form of nicotinamide adenine dinucleotide (NAD^+)

et al., 2003) and with the constant concentration observed in this study between p29 and p77 in the hippocampus and between p35 and p77 in the cerebellum. This also corroborates previous studies showing constant Gln concentration in the brain between p28/p30 and adulthood (Bayer & McMurray, 1967; Oja & Piha, 1966; Oja et al., 1968) measured by ex vivo chromatographic, spectrophotometric or other biochemical methods. In contrast, Burri et al. (Burri et al., 1990) showed in brain extracts a slight increase in Gln between p35 and adulthood, measured by in vitro ^{1}H MRS and chromatography.

This study showed that **Glu** increased in the hippocampus (mostly until p49) but not in the cerebellum. The measured increase in the hippocampus was consistent with the work of others (Burri et al., 1990; Oja & Piha, 1966; Oja et al., 1968) who described an increase in whole-brain Glu between p30/p35 and adult rat using ex vivo methods. However, Bayer et al. reported a rather constant brain Glu concentration between p29 and adults (Bayer & McMurray, 1967), possibly due to the measurements in the cerebrum and cerebellum. It is important to emphasize that a precise comparison with other studies is difficult because of methodological differences and anatomical regions studied. Finally, in this study, we did not observe any significant change in **Asp** and **GABA** concentration in the hippocampus or the cerebellum.

4.2 | Metabolites involved in phospholipid metabolism

PCho, GPC, PE, GPE but also **Ins** are anabolic or catabolic products of phospholipids. They are a source of choline, ethanolamine and inositol for phospholipid synthesis and therefore play an important role in membrane metabolism and myelination. Phospholipids are essential both for membrane remodelling and synthesis and for signal transduction. Choline-containing compounds serve as precursors for the neurotransmitter acetylcholine, and Ins acts as a precursor for second messengers.

Phospholipids are essential during brain development because of intense cell membrane turnover and myelination. Phospholipid turnover is elevated at birth and increases by 30% by adulthood, indicating its importance early in brain development (Carey & Foster, 1984). In addition, different phospholipid species show diverse patterns during post-natal development (Carey & Foster, 1984).

In this study, we showed constant **PE** concentrations in both the hippocampus and cerebellum. We also observed a significant increase in **tCho** in the hippocampus between p29 and p77, whereas in the cerebellum tCho did not change significantly between p35 and p77. tCho resonances in ^{1}H MRS include several choline-containing compounds, mainly PCho and GPC. Through the use of ^{31}P MRS we concluded that the observed increase in tCho by ^{1}H MRS in hippocampus was due to GPC increase. The constant PE concentration observed in the hippocampus was also confirmed by ^{31}P MRS in a larger VOI covering cortex, hippocampus and striatum.

Several studies have reported a decrease in PE between p7 and p28, (Burri et al., 1988, 1990; Tkáč et al., 2003), a decrease in phospho-monoesters (PE + PCho) (Burri et al., 1988; Hida et al., 1992; Tofts & Wray, 1985) or decrease in tCho (Hida et al., 1992; Tkáč et al., 2003). These changes were measured by ^{1}H MRS or ^{31}P MRS, mainly in whole brain or different brain regions including the hippocampus but not the cerebellum. The sudden switch between: (1) the decrease in PE and tCho during the

FIGURE 4 **Evolution of brain metabolites measured by in vivo longitudinal ^{1}H MRS in hippocampus** p29 (n = 7), p35 (n = 7), p43 (n = 7), p49 (n = 7), p57 (n = 7), p63 (n = 7), p71 (n = 7), p77 (n = 7). Alanine (Ala), ascorbate (Asc), aspartate (Asp), creatine (Cr), phosphocreatine (PCr), γ-aminobutyric acid (GABA), glutamine (Gln), glutamate (Glu), glutathione (GSH), myo-Inositol (Ins), lactate (Lac), N-acetylaspartate (NAA), N-acetylaspartylglutamate (NAAG), phosphoethanolamine (PE), total choline (tCho), taurine (Tau), n represents the number of animals per group

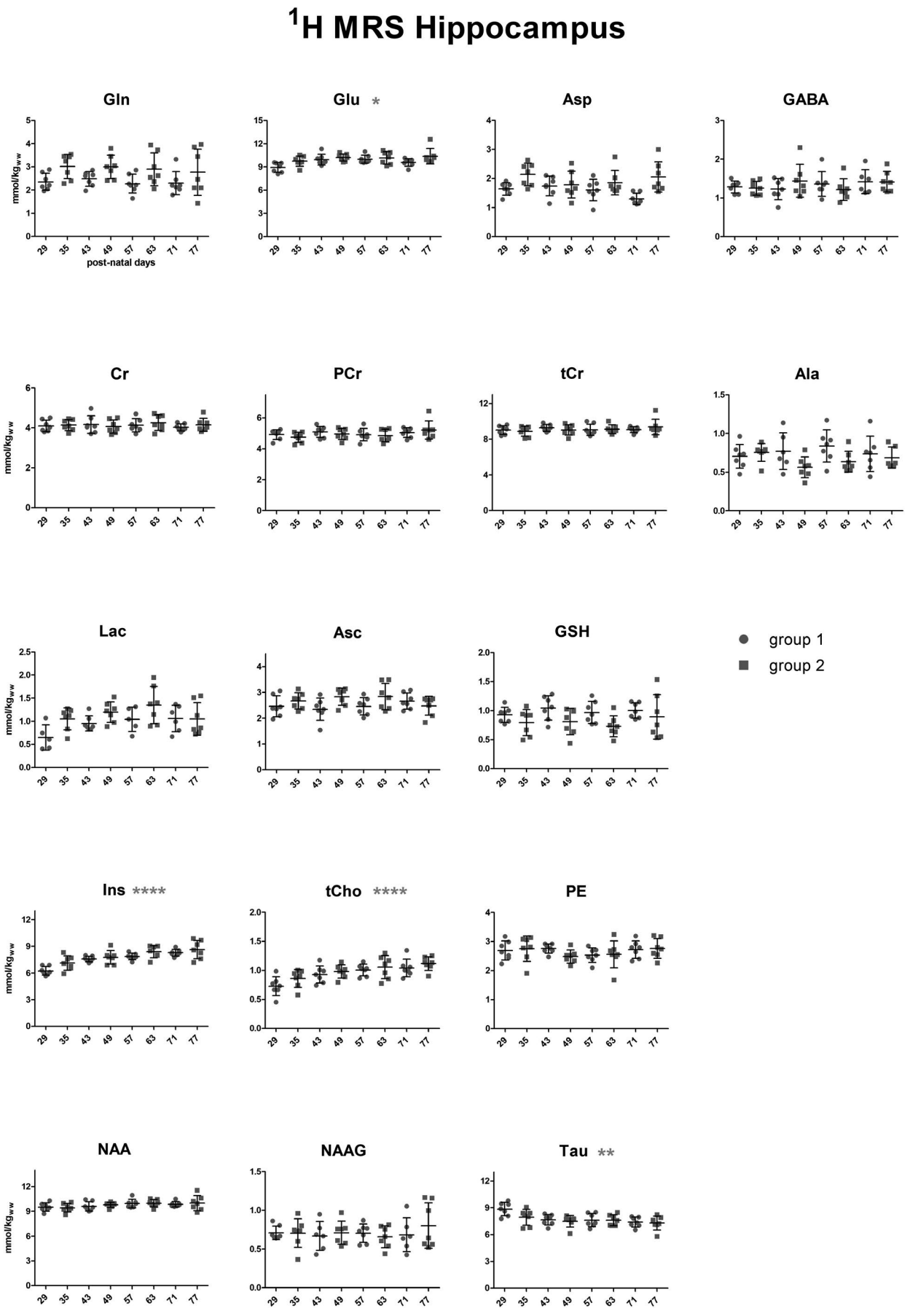
1H MRS Hippocampus
Gln
Glu *
Asp
GABA
Cr
PCr
tCr
Ala
Lac
Asc
GSH
Ins ****
tCho ****
PE
NAA
NAAG
Tau **
mmol/kgww
post-natal days
29 35 43 49 57 63 71 77
group 1
group 2

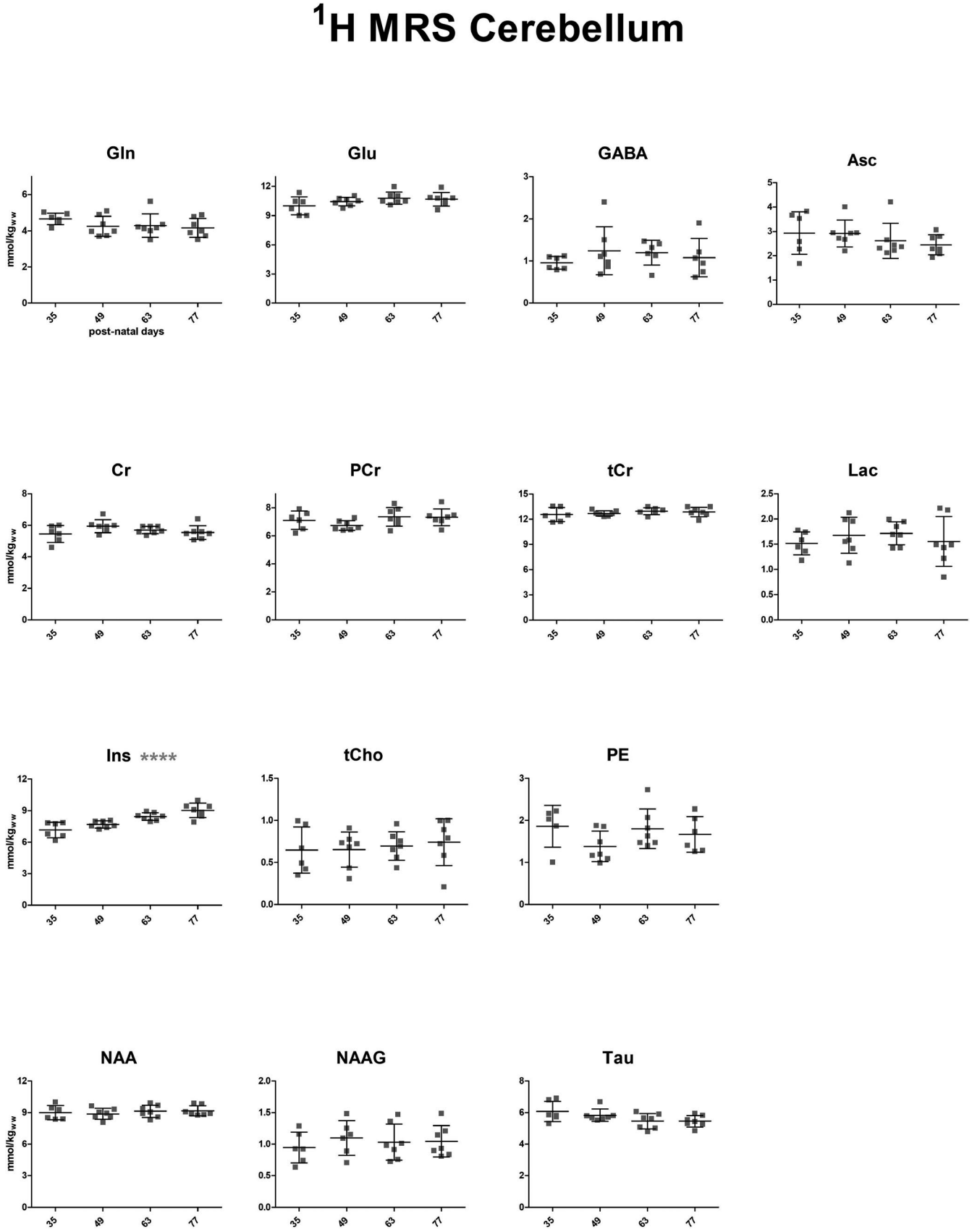

FIGURE 5 **Evolution of brain metabolites measured by in vivo longitudinal ^{1}H MRS in cerebellum.** p35 ($n = 6$), p49 ($n = 7$), p63 ($n = 7$), p77 ($n = 7$). Ascorbate (Asc), aspartate (Asp), creatine (Cr), phosphocreatine (PCr), γ-aminobutyric acid (GABA), glutamine (Gln), glutamate (Glu), myo-Inositol (Ins), lactate (Lac), N-acetylaspartate (NAA), N-acetylaspartylglutamate (NAAG), phosphoethanolamine (PE), total choline (tCho), taurine (Tau), n represents the number of animals per group

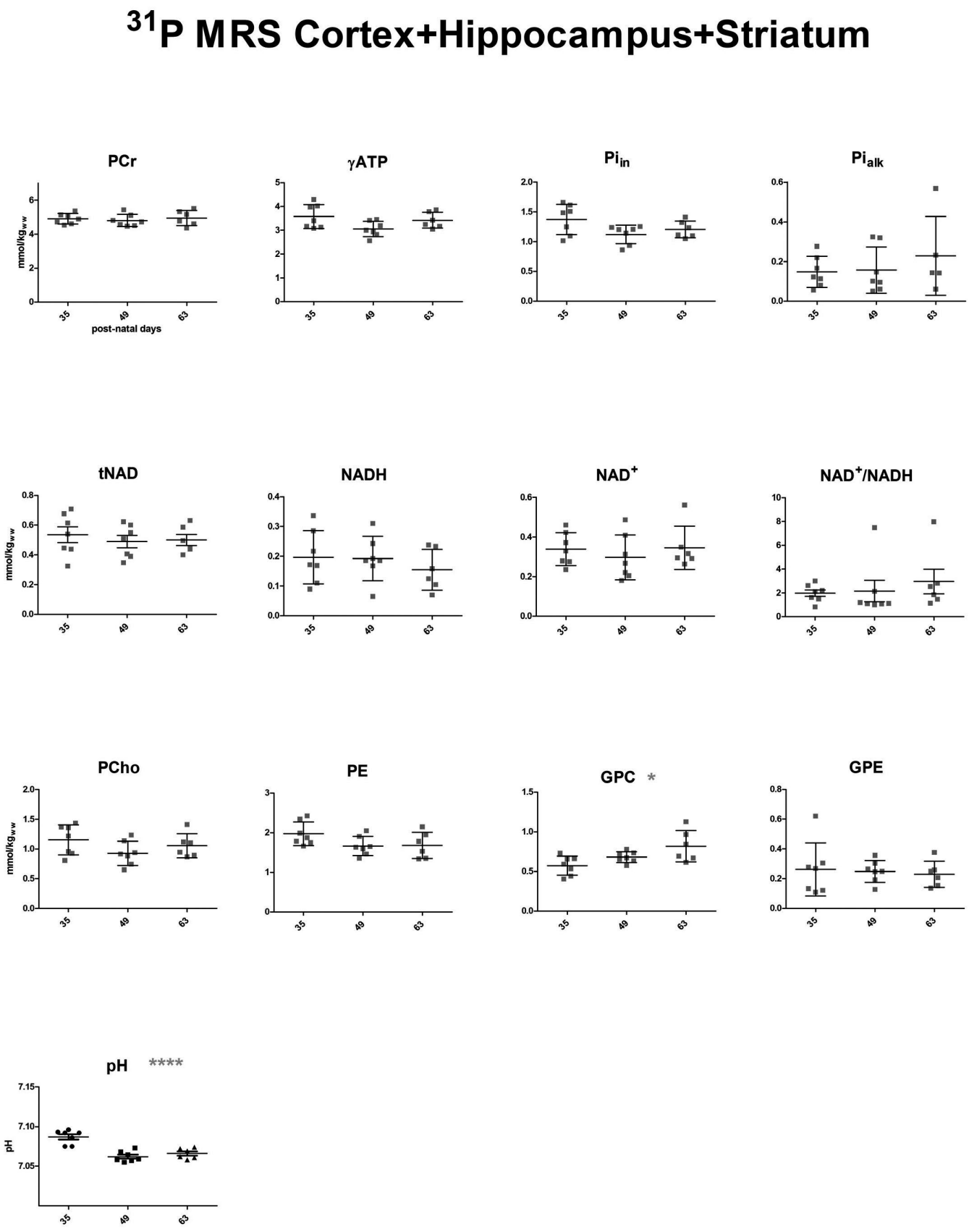

FIGURE 6 **Evolution of brain metabolites measured by in vivo longitudinal ^{31}P MRS in VOI = 5 × 9 × 9 mm^3.** p35 (n = 7), p49 (n = 7), p63 (n = 6). Phosphocreatine (PCr), gamma-phosphorus in adenosine tri-phosphate (γATP), alkaline and intracellular inorganic phosphate (Pi_{alk} and Pi_{in}), total nicotinamide adenine dinucleotide (tNAD), reduced form of nicotinamide adenine dinucleotide (NADH), oxidized form of nicotinamide adenine dinucleotide (NAD^+), phosphocholine (PCho), phosphoethanolamine (PE), glycerophosphocholine (GPC), glycerophosphoethanolamine (GPE), n represents the number of animals per group

early post-natal period until p28 observed in other studies and (2) the constant PE with increasing tCho in the hippocampus (or more precisely increasing GPC) after p29 observed in our study might be related to changes in cell density and ratio between neuronal and non-neuronal cells in the early and later post-natal periods (maturation and changes in the density of axons as well as branches and spines on dendritic trees, and in astrocytic processes). Bandeira et al. have reported a decrease in neuronal density and an increase in non-neuronal cell density between birth and p20 in the hippocampus, resulting in increase in non-neuronal to neuronal cells ratio during this period and stabilizing thereafter (Bandeira et al., 2009).

The switch in concentrations of metabolites involved in phospholipid metabolism in the hippocampus around p28 might also be related to different rates of myelination before and after ≈p25. Studies have shown that the maximum myelination in the rat brain, including in the hippocampus, takes place during the period between p10 and ≈p25 (Jacobson, 1963; Meier et al., 2004; Wiggins, 1986). This interval of intense myelination is followed by a period of slow myelination (Wiggins, 1982; Rice and Barone 2000) and with age-dependent changes in myelin composition (Smith, 1973).

In addition, Huxtable et al. have shown a sharp decrease in phosphatidyl-choline and phosphatidyl-ethanolamine (phospholipids unmeasurable by MRS) in synaptosomes until p28 followed by a slight increase between p28 and p56 which correlates with our findings in the hippocampus (Huxtable et al., 1989).

It has been previously shown that **Ins** concentration increases from birth until p28 (Tkáč et al., 2003). Our study adds to this previous report by demonstrating that Ins concentrations continued to rise both in the hippocampus and cerebellum, at least until p77. This increase may be linked to membrane formation and myelination, in both areas, given that Ins is a precursor of phosphatidyl-inositol. Polyphospho-inosides are an important component of myelin and contribute significantly to myelin phospholipid turnover both in the adult and the developing brain (Jungalwala & Dawson, 1971). Uma et al. reported that some polyphospho-inosides increased in the rat brain until p34, whereas some increased until p63 and beyond (Uma & Ramakrishnan, 1983).

Therefore, the observed increases in tCho and Ins in the hippocampus may be related given that both are involved in phospholipid metabolism. Finally, while the Ins increase was accompanied by tCho increase in the hippocampus, this was not observed in the cerebellum between p35 and p77.

4.3 | Taurine

A post-natal decrease in brain **Tau** concentration is accepted to be an important neurodevelopmental event and is highly conserved across species (Huxtable, 1992). Tau decrease takes place in spite of increasing cysteine sulphinate decarboxylase activity from birth to adulthood (Agrawal et al., 1971). Therefore, it is believed that this Tau decrease might be because of a loss of maternal Tau stores (Agrawal et al., 1971; Sturman et al., 1977). In this study, a significant decrease in Tau between p29 and p77 (with sharper decrease until p49) was observed in the hippocampus , in agreement with previous studies performed between p28/p30 and adulthood (Agrawal et al., 1971; Huxtable et al., 1989; Oja & Piha, 1966; Oja et al., 1968). The small but non-significant decrease in Tau observed in the cerebellum between p35 and p77 suggests that the sharp decline in Tau was already passed. Tau has a similar molecular shape and charge to phosphatidyl-choline and phosphatidyl-ethanolamine and therefore can interact with membranes, meaning that the decrease in Tau during development observed in the hippocampus in our study can play a role in membrane stabilization. Moreover, Tau appears to regulate the ratio between ethanolamine and choline in some membranes, probably by regulating the rate of phospholipid methylation (Huxtable, 1992; Huxtable et al., 1989). This is in line with the significant changes in both Tau and tCho in the hippocampus observed in this study. The ethanolamine to choline ratio will influence membrane structure and properties because phosphatidyl-choline is preferentially localized on the outer part of phospholipid bilayer and phosphatidylethanolamine is preferentially on the inner part (Deleke, 2007; Harper et al., 2014; Ikeda et al., 2006; Schaffer et al., 1995). Of note, it was sugested based on in vivo and ex vivo ^{1}H MRS experiments in rats until ~p30 that Tau in fetal brain is the counterpart of NAA in adult brain (Nakada, 2010).

4.4 | Metabolites involved in energy metabolism

Metabolites involved in energy metabolism did not present any significant changes during the observation period up to p77 in any of the brain region studied (Cr, PCr, γATP, Pi_{in}). Cr and PCr were shown to increase in rat brain during post-natal period (Burri et al., 1990; Hida et al., 1992; Tkáč et al., 2003; Tofts & Wray, 1985), and our data showed that these stay stable after p29 in the hippocampus and after p35 in the cerebellum. This is important information for in vivo MRS studies that often use tCr (in ^{1}H MRS) or PCr (in ^{31}P MRS) as an internal concentration reference. No change in ATP was expected as adult levels of adenine nucleotides are expected to be reached early during brain development (Erecinska et al., 2004).

It has to be emphasized that mammalian species develop at different rates especially when focusing on neurodevelopmental processes and brain regions. As such, finding the exact 'equivalence' between species for a specific neurodevelopmental process, and then establishing when all neurodevelopmental processes in rats at a specific moment translate in a specific time window in humans, is very complex and it may only be considered as far as a specific event or function is concerned (Erecinska et al., 2004). In the present work, we used as reference a model of brain developmental characteristics across mammalian species (Workman et al., 2013; http://translatingtime.org/translate) where rat brain development at p29 is considered to correspond to ≈1.5-year-old human taking into account most of developmental features (myelination, axonal growth, neurogenesis, sensorimotor development and brain growth). In other manuscripts, the rodent brain

at p20-21 has been considered to correspond to a 2–3 years old human (Semple et al., 2013).

In conclusion, the results of this study provide insight into the neurometabolic changes during the late phases of brain development in the male rat (post-natal period p29/p35 - p77) both in the hippocampus and cerebellum. Rat animal models are widely used in research, especially young adult rats, and physiological changes in brain metabolites may impact data interpretation during certain developmental windows. In the hippocampus, our results provide compelling evidence to suggest that the dominant metabolic developmental feature during this period involves phospholipid metabolism, membrane formation and myelination, as both tCho and Ins play a role as phospholipids precursors or degradation products. In addition, sustained Glu increase and Tau decrease were also observed, both previously known to occur earlier during post-natal development. In the cerebellum, the only significant change was an increase in Ins. Finally, there were no significant changes in energy metabolism during the studied window as measured by Cr, PCr, ATP or Pi_{in}. We propose that these late changes are the signature of late enzymatic maturation (Bayer & McMurray, 1967).

ACKNOWLEDGEMENTS

The authors thank the veterinary team at CIBM for support during experiments. We acknowledge access to the facilities and expertise of the CIBM Center for Biomedical Imaging, a Swiss research center of excellence founded and supported by Lausanne University Hospital (CHUV), University of Lausanne (UNIL), Ecole Polytechnique Fédérale de Lausanne (EPFL), University of Geneva (UNIGE) and Geneva University Hospitals (HUG). **Funding support** was provided by the SNSF project no 310030_173222, the EU: FP7-PEOPLE-2012-ITN project 316679 TRANSACT and by the CIBM (UNIL, UNIGE, HUG, CHUV, EPFL, as well as the Leenaards and Jeantet Foundations), the CHUV and the HUG.

All experiments were conducted in compliance with the ARRIVE guidelines.

CONFLICT OF INTEREST

The authors have declared that no conflict of interest exists.

DATA AVAILABILITY STATEMENT

The datasets generated during and/or analysed during this study are available from the corresponding author on reasonable request.

ORCID

Olivier Braissant https://orcid.org/0000-0002-8068-3344
Rolf Gruetter https://orcid.org/0000-0003-1870-4025
Valérie A. McLin https://orcid.org/0000-0002-0711-687X
Cristina Cudalbu https://orcid.org/0000-0003-4582-2465

REFERENCES

Agrawal, H. C., Davison, A. N., & Kaczmarek, L. K. (1971). Subcellular distribution of taurine and cysteinesulphinate decarboxylase in developing rat brain. *The Biochemical Journal*, *122*, 759–763.

Altman, J. (1972a). Postnatal development of the cerebellar cortex in the rat. I. The external germinal layer and the transitional molecular layer. *The Journal of Comparative Neurology*, *145*, 353–397. https://doi.org/10.1002/cne.901450305

Altman, J. (1972b). Postnatal development of the cerebellar cortex in the rat. III. Maturation of the components of the granular layer. *The Journal of Comparative Neurology*, *145*, 465–513. https://doi.org/10.1002/cne.901450403

Altman, J. (1972c). Postnatal development of the cerebellar cortex in the rat. II. Phases in the maturation of Purkinje cells and of the molecular layer. *The Journal of Comparative Neurology*, *145*, 399–463. https://doi.org/10.1002/cne.901450402

Altman, J., & Das, G. D. (1965). Autoradiographic and histological evidence of postnatal hippocampal neurogenesis in rats. *The Journal of Comparative Neurology*, *124*, 319–335.

Altman, J., & Das, G. D. (1966). Autoradiographic and histological studies of postnatal neurogenesis. I. A longitudinal investigation of the kinetics, migration and transformation of cells incoorporating tritiated thymidine in neonate rats, with special reference to postnatal neurogenesi. *The Journal of Comparative Neurology*, *126*, 337–389.

Bandeira, F., Lent, R., & Herculano-Houzel, S. (2009). Changing numbers of neuronal and non-neuronal cells underlie postnatal brain growth in the rat. *Proceedings of the National Academy of Sciences of the United States of America*, *106*, 14108–14113.

Bayer, S. A., Altman, J., Russo, R. J., & Zhang, X. (1993). Timetables of neurogenesis in the human brain based on experimentally determined patterns in the rat. *Neurotoxicology*, *14*, 83–144.

Bayer, S. M., & McMurray, W. C. (1967). The Metabolism of amino acids in developing rat brain. *Journal of Neurochemistry*, *14*, 695–706. https://doi.org/10.1111/j.1471-4159.1967.tb10303.x

Burri, R., Bigler, P., Straehl, P., Posse, S., Colombo, J.-P., & Herschkowitz, N. (1990). Brain development: 1H magnetic resonance spectroscopy of rat brain extracts compared with chromatographic methods. *Neurochemical Research*, *15*, 1009–1016. https://doi.org/10.1007/BF00965747

Burri, R., Lazeyras, F., Aue, W. P., Straehl, P., Bigler, P., Althaus, U., & Herschkowitz, N. (1988). Correlation between 31P NMR phosphomonoester and biochemically determined phosphorylethanolamine and phosphatitylethanolamine during development of the rat brain. *Developmental Neuroscience*, *10*, 213–221.

Carey, E. M., & Foster, C. (1984). Phospholipid exchange activity in developing rat brain. *Biochimica Et Biophysica Acta*, *792*, 48–58.

Cudalbu, C., Mlynárik, V., & Gruetter, R. (2012). Handling macromolecule signals in the quantification of the neurochemical profile. *Journal of Alzheimer's Disease*, *31*(Suppl 3), S101–S115. https://doi.org/10.3233/JAD-2012-120100

De, S. S. W., & Dobbing, J. (1971). Cerebral water rat edema and in developing cation brain: I. normal content postmortem in developing changes. *Experimental Neurology*, *32*, 431–438.

Deleke, D. (2007). Phospholipid Flippases. *Journal of Biological Chemistry*, *282*(2), 821–825.

Erecinska, M., Cherian, S., & Silver, I. A. (2004). Energy metabolism in mammalian brain during development. *Progress in Neurobiology*, *73*, 397–445.

Gruetter, R. (1993). Automatic, localized in vivo adjustment of all first- and second-order shim coils. *Magnetic Resonance in Medicine*, *29*, 804–811.

Gruetter, R., & Tkác, I. (2000). Field mapping without reference scan using asymmetric echo-planar techniques. *Magnetic Resonance in Medicine*, *43*, 319–323.

Harper, D. G., Jensen, J. E., Ravichandran, C., Sivrioglu, Y., Silveri, M., Iosifescu, D. V., Renshaw, P. F., & Forester, B. P. (2014). Tissue-specific differences in brain phosphodiesters in late-life major depression. *American Journal of Geriatric Psychiatry*, *22*, 499–509.

Hida, K., Kwee, I. L., & Nakada, T. (1992). In vivo 1H and 31P NMR spectroscopy of the developing rat brain. *Magnetic Resonance in Medicine*, *23*, 31–36. https://doi.org/10.1002/mrm.1910230105

Huxtable, R. J. (1992). Physiological actions of taurine. *Physiological Reviews*, *72*(1), 101–163.

Huxtable, R. J., Crosswell, S., & Parker, D. (1989). Phospholipid composition and taurine content of synaptosomes in developing rat brain. *Neurochemistry International*, *15*, 233–238. https://doi.org/10.1016/0197-0186(89)90106-X

Ikeda, M., Kihara, A., & Igarashi, Y. (2006). Lipid asymmetry of the eukaryotic plasma membrane: Functions and related enzymes. *Biological &/and Pharmaceutical Bulletin*, *29*, 1542–1546. https://doi.org/10.1248/bpb.29.1542

Jacobson, S. (1963). Sequence of myelinization in the brain of the albino rat. *The Journal of Comparative Neurology*, *121*, 5–29.

Jungalwala, F. B., & Dawson, R. M. (1971). The turnover of myelin phospholipids in the adult and developing rat brain. *The Biochemical Journal*, *123*, 683–693.

Lanz, B., Rackayova, V., Braissant, O., & Cudalbu, C. (2017). MRS studies of neuroenergetics and glutamate/glutamine exchange in rats: Extensions to hyperammonemic models. *Analytical Biochemistry*, *529*, 245–269. https://doi.org/10.1016/j.ab.2016.11.021

Leong, S. F., & Clark, J. B. (1984a). Regional enzyme development in rat brain. Enzymes of energy metabolism. *Biochemical Journal*, *218*, 139–145. https://doi.org/10.1042/bj2180139

Leong, S. F., & Clark, J. B. (1984b). Regional enzyme development in rat brain. Enzymes associated with glucose utilization. *The Biochemical Journal*, *218*, 131–138. https://doi.org/10.1042/bj2180131

Mckenna, M. C., Scafidi, S., & Robertson, C. L. (2015). Metabolic alterations in developing brain after injury: Knowns and unknowns. *Neurochemical Research*, *40*, 2527–2543.

Meier, S., Bräuer, A. U., Heimrich, B., Nitsch, R., & Savaskan, N. E. (2004). Myelination in the hippocampus during development and following lesion. *Cellular and Molecular Life Sciences*, *61*, 1082–1094.

Mlynárik, V., Cacquevel, M., Sun-Reimer, L., Janssens, S., Cudalbu, C., Lei, H., Schneider, B. L., Aebischer, P., & Gruetter, R. (2012). Proton and phosphorus magnetic resonance spectroscopy of a mouse model of Alzheimer's disease. *Journal of Alzheimer's Disease*, *31*, S87–S99. https://doi.org/10.3233/JAD-2012-112072

Mlynárik, V., Gambarota, G., Frenkel, H., & Gruetter, R. (2006). Localized short-echo-time proton MR spectroscopy with full signal-intensity acquisition. *Magnetic Resonance in Medicine*, *56*, 965–970.

Nakada, T. (2010). Conversion of brain cytosol profile from fetal to adult type during the perinatal period: Taurine-NAA exchange. *Proc. Japan Acad. Ser. B Phys. Biol. Sci.*, *86*, 630–642.

Oja, S. S., & Piha, R. S. (1966). Changes in the concentration of free amino acid in the rat brain during postnatal development. *Life Sciences*, *5*, 865–870.

Oja, S. S., Uusitalo, A. J., Vahvelainen, M. L., & Piha, R. S. (1968). Changes in cerebral and hepatic amino acids in the rat and guinea pig during development. *Brain Research*, *11*, 655–661. https://doi.org/10.1016/0006-8993(68)90153-4

Provencher, S. W. (2001). Automatic quantitation of localized in vivo 1H spectra with LCModel. *NMR in Biomedicine*, *14*, 260–264. https://doi.org/10.1002/nbm.698

Rackayova, V., Braissant, O., McLin, V. A., Berset, C., Lanz, B., & Cudalbu, C. (2016). 1H and 31P magnetic resonance spectroscopy in a rat model of chronic hepatic encephalopathy: In vivo longitudinal measurements of brain energy metabolism. *Metabolic Brain Disease*, *31*, 1303–1314. https://doi.org/10.1007/s11011-015-9715-8

Rice, D., & Barone, S. Jr (2000). Critical periods of vulnerability for the developing nervous system: evidence from humans and animal models. *Environmental Health Perspectives*, *108*, 511–533.

Schaffer, S. W., Azuma, J., & Madura, J. D. (1995). Mechanisms underlying taurine-mediated alterations in membrane function. *Amino Acids*, *8*, 231–246. https://doi.org/10.1007/BF00806821

Semple, B. D., Blomgren, K., Gimlin, K., Ferriero, D. M., & Noble-Haeusslein, L. J. (2013). Brain development in rodents and humans: Identifying benchmarks of maturation and vulnerability to injury across species. *Progress in Neurobiology*, *106–107*, 1–16. https://doi.org/10.1016/j.pneurobio.2013.04.001

Smith, M. E. (1973). A regional survey of myelin development: Some compositional and metabolic aspects. *Journal of Lipid Research*, *14*, 541–551. https://doi.org/10.1016/S0022-2275(20)36859-0

Sturman, J. A., Rassin, D. K., & Gaull, G. E. (1977). Taurine in developing rat brain: Maternal-fetal transfer of [35 S] taurine and its fate in the neonate. *Journal of Neurochemistry*, *28*, 31–39.

Terpstra, M., Andersen, P. M., & Gruetter, R. (1998). Localized eddy current compensation using quantitative field mapping. *Journal of Magnetic Resonance*, *131*, 139–143.

Terpstra, M., Rao, R., & Tkac, I. (2010). Region-specific changes in ascorbate concentration during rat brain development quantified by in vivo 1H NMR spectroscopy. *NMR in Biomedicine*, *23*, 1038–1043. https://doi.org/10.1002/nbm.1528

Tkáč, I., Rao, R., Georgieff, M. K., & Gruetter, R. (2003). Developmental and regional changes in the neurochemical profile of the rat brain determined by in vivo 1H NMR spectroscopy. *Magnetic Resonance in Medicine*, *50*, 24–32.

Tkáč, I., Starčuk, Z., Choi, I. Y., & Gruetter, R. (1999). In vivo 1H NMR spectroscopy of rat brain at 1 ms echo time. *Magnetic Resonance in Medicine*, *41*, 649–656.

Tofts, P., & Wray, S. (1985). Changes in brain phosphorus metabolites during the post-natal development of the rat. *Journal of Physiology*, *359*, 417–429. https://doi.org/10.1113/jphysiol.1985.sp015593

Uma, S., & Ramakrishnan, C. V. (1983). Studies on polyphosphoinositides in developing rat brain. *Journal of Neurochemistry*, *40*, 914–916. https://doi.org/10.1111/j.1471-4159.1983.tb08073.x

Vanhamme, L., van den Boogaart, A., & Van, H. S. (1997). Improved method for accurate and efficient quantification of MRS data with use of prior knowledge. *Journal of Magnetic Resonance*, *129*, 35–43.

Wiggins, R. C. (1982). Myelin development and nutritional insufficiency. *Brain Research Reviews*, *4*, 151–175.

Wiggins, R. C. (1986). Myelination: A critical stage in development. *Neurotoxicology*, *7*, 103–120.

Workman, A. D., Charvet, C. J., Clancy, B., Darlington, R. B., & Finlay, B. L. (2013). Modeling transformations of neurodevelopmental sequences across mammalian species. *Journal of Neuroscience*, *33*, 7368–7383. https://doi.org/10.1523/JNEUROSCI.5746-12.2013

SUPPORTING INFORMATION

Additional supporting information may be found online in the Supporting Information section.

How to cite this article: Račkayová V, Simicic D, Donati G, et al. Late post-natal neurometabolic development in healthy male rats using ^{1}H and ^{31}P magnetic resonance spectroscopy. *J Neurochem*. 2021;00:1–12. https://doi.org/10.1111/jnc.15294